

# Remote weather associated with North Pacific subtropical sea-level high properties

Richard Grotjahn\* and Muhtarjan Osman

*Department of Land, Air, and Water Resources, University of California, Davis CA 95616 USA*

## Abstract:

Remote events influencing North Pacific (NP) subtropical high properties in monthly and daily data are identified. Variability in the NP during summer is far more strongly dominated by midlatitude events than in South Pacific (SP); low-pass filtering is required to see tropical associations.

The dominant pattern in composites, correlations, and regressions is a midlatitude wave train. A stronger NP high was led by higher sea-level pressure (SLP) just east of Japan and lower SLP over central Canada and to a lesser extent over western tropical Pacific.

Various mechanisms have been proposed to force the NP high:

- (1) Heating over southwestern North America (with cooling off the west coast). However, higher temperatures over North America follow stronger SLP over the NP high and occur much further east than postulated. Higher SLP occurs where temperatures are lower over western North America and adjacent ocean. Thermal pattern is consistent with temperature advection between NP high and Canadian low.
- (2) Precipitation over and near Central America. However, SLP increase on the SE side of the high is led by higher SLP (and *higher* outgoing longwave radiation (OLR)) along the west coast of Mexico and Central America. Normalized regressions find a very weak lower OLR in North American monsoon preceding stronger NP high, but the region is much smaller in size and magnitude than other significant areas.
- (3) Precipitation over Indonesia and southeast Asia. Statistics provide some support for lower SLP and OLR over Indonesia preceding higher SLP in the center, west, and northwest sides of NP high. The lower SLP and OLR appear to migrate into southeast Asia, perhaps independently, perhaps from stronger NP high.
- (4) The NP high has a strong connection to El Niño during winter, but no significant link during summer. Only the south side of NP high appears (weakly) linked to the Madden Julian oscillation (MJO). Copyright © 2006 Royal Meteorological Society

KEY WORDS subtropical highs; sea-level pressure SLP; MJO; ENSO; regressions; correlations; composites; North Pacific

*Received 17 June 2006; Revised 1 August 2006; Accepted 5 August 2006*

## INTRODUCTION

This is the second in a series of papers on observed associations between subtropical high properties and remote events that may be expected to influence the subtropical high in sea-level pressure (SLP). The first paper, Grotjahn (2004), focused upon associating variations of remote events with variations of the South Pacific subtropical high (hereafter SP high). This paper is an analogous study of the subtropical high of the North Pacific (hereafter NP high). The earlier work demonstrated that the SLP variations on a given side of the SP high lagged forcing on that side, in general. The SLP on the west and southern sides of the SP high responded to the Southern Hemisphere midlatitude forcing linked to the traveling extratropical highs and lows. SLP on the north and northeast sides of

the SP high was greater after both expansion of the Amazonian convection and lessening of convection over New Guinea and northern Australia regions.

Before discussing some prior work and working hypotheses a few facts are useful. On a zonal average the subtropical highs are strongest in winter (Figure 1(a)). The winter maximum seems consistent with the zonal mean, 'Hadley' circulation being strongest then as well. The zonal mean SLP includes lower than annual average pressure over land areas in summer and a more zonally uniform SLP pattern in winter. So, when the zonal mean is not taken, seasonal (or monthly) averages find the North Pacific (NP) and North Atlantic highs stronger in summer (Figure 1(b), (c)). The Northern Hemisphere seasonal change has led some to conclude erroneously that all the subtropical highs are strongest in summer. They are not. The South Pacific (SP high) is strongest in the local springtime (Figure 1(e)). The subtropical highs of the southern Indian and Atlantic oceans are strongest in

\* Correspondence to: Richard Grotjahn, Department of Land, Air, and Water Resources, University of California, Davis CA 95616 USA.  
E-mail: grotjahn@ucdavis.edu

winter. (Figure 1(d), (f)). Surface highs are often associated with colder lower tropospheric temperatures. Hence, the North Atlantic high is often hard to distinguish from strong high pressure over northwestern North Africa, Spain, and elsewhere in Europe during winter. Clearly, the subtropical highs do not all have the same climatology.

Most research on the subtropical highs has occurred in the past decade. Hoskins (1996) and subsequent papers (see Shaffrey *et al.*, 2002, for a list of references) advanced the idea that the summertime intensification of the Northern Hemisphere subtropical highs is a nonlinear response to tropical diabatic (latent) heating to the east and equatorward of those highs. In their later papers they emphasize the major topographic features as well. For example, Rodwell and Hoskins (2001) drive a primitive equations (PE) model with diabatic heating deduced as a thermodynamic equation residual. They terminate their calculation before transient midlatitude eddies become established. Rodwell and Hoskins do not further partition the diabatic heating field into different contributors. In contrast, Chen *et al.* (2001) input diabatic heating from idealized deep monsoonal convection west of each high into a linearized quasi-geostrophic model. Chen *et al.* obtain a baroclinic stationary wave with low SLP over Asia and North America and higher SLP over the oceans with opposite sign for that wave in the upper troposphere. The sign reversal is observed in the zonally asymmetric part of the geopotential height field. Liu *et al.* (2004) emphasize another part of the diabatic heating field. Liu *et al.* find that shallow near-surface diabatic heating, both continental heating east of the high and oceanic cooling near the high, leads to subtropical high formation. Isentropic ‘potential vorticity

PV thinking’ would predict low-level high pressure associated with a surface cold anomaly and a low for a warm anomaly. Seager *et al.* (2003) conclude that local air–sea interaction is needed as well to provide sufficient intensification of the subtropical high. Low-level equatorward flow on the eastern flank of the high causes upwelling and colder sea-surface temperatures (SST) (leading to low-level atmosphere stabilization, stratiform clouds, and negative net radiation). Poleward flow on the *western* side of the high advects warm SSTs poleward, destabilizing the atmosphere and allowing convection to spread eastward, enhancing further the zonally asymmetric heating. Miyasaka and Nakamura (2005) use a combination of observations and PE model to investigate several of these mechanisms. Miyasaka and Nakamura (2005) find comparatively little response from the monsoonal deep convective heating emphasized by the Rossby wave proponents (e.g. Rodwell and Hoskins, 2001) in their interpretation, but instead isolate the importance of lower tropospheric heating emphasized by others (and also present in studies like Rodwell and Hoskins, 2001).

Observations and simple theory provide a context to understand some of the subtropical high forcing. Miyasaka and Nakamura (2005) show that the zonally asymmetric part of the tropospheric relative vorticity has a complex pattern above the NP. The relative vorticity is equivalent-barotropic on the north side of the high and baroclinic on the south side. That vorticity pattern follows from a large surface subtropical high with the upper level horizontal shear of two subtropical jets. The jet to the north is the decelerating ‘jet exit’ portion of the East Asian subtropical jet. The jet to the south is partly the accelerating ‘jet entrance’ region of the North American

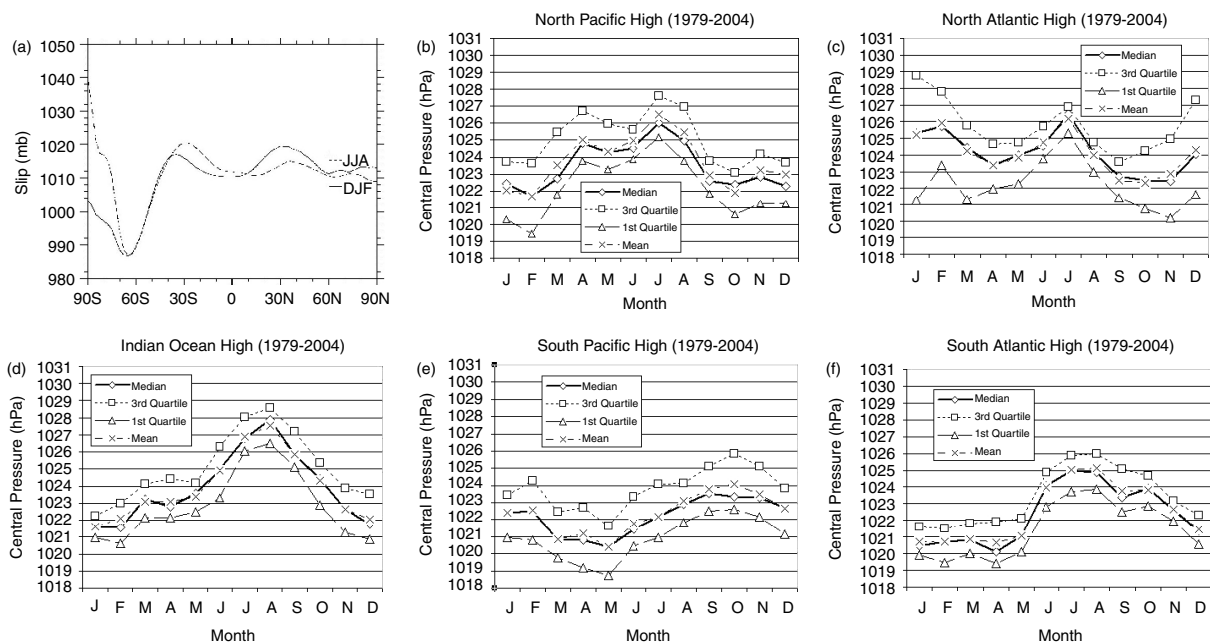


Figure 1. Subtropical high climatology. (a) Zonal mean sea-level pressure (SLP) for December–February and June–August using 1979–2004 data. Mean and first through third quartiles of SLP for five subtropical highs, by month: (b) NP high, (c) North Atlantic high, (d) southern Indian Ocean high, (e) SP high, (f) South Atlantic high.

subtropical jet. In turn, the zonal acceleration and deceleration of these time-mean jets may be largely balanced by ageostrophic meridional flux of planetary vorticity. This long-held simplification balances two terms of the zonal momentum equation (Namias and Clapp, 1947). Convergence of these upper level ageostrophic winds produces sinking above and on the eastern side of the subtropical highs. As mentioned, Grotjahn (2004) introduced consideration of extratropical cyclone/anticyclone forcing. One sees that connection by recognizing that those upper level equatorward ageostrophic winds arise from maintaining thermal wind balance for developing frontal cyclones. Hence, this picture provides a connection between the subtropical SLP high and the frontal cyclones. On the east side of the NP high, the vorticity equation might be simplified (Hoskins, 1996) to a balance between planetary vorticity advection and the divergence term. Such a balance where there is low-level divergence (from downward motion that decreases as pressure increases) implies southward motion. Surface northerlies near the west coast of North America can drive water offshore, thereby upwelling much colder water. This mechanism lowers surface temperatures, consistent with a SLP high based on 'PV thinking'. The above information suggests a simple conceptual model for the NP high in summer, shown in Figure 2.

#### DATA AND ANALYSIS TOOLS

The data and data analysis tools are similar to Grotjahn (2004). Therefore, only brief descriptions of the data and analysis methods are listed here. The primary difference from before is that time filtering is needed in this study.

NCEP/NCAR reanalysis data are used (see Kalnay *et al.*, 1996; Kistler *et al.*, 2001). The data were provided by the NOAA-CIRES Climate Diagnostics Center

(CDC), Boulder, Colorado, USA, from their web site at <http://www.cdc.noaa.gov/>. Only data supplemented by satellite measurements are used, that is, starting with January 1979. Precipitation and interpolated outgoing longwave radiation (OLR) data were also obtained from the CDC-NOAA website. Monthly data were discussed at the 13th conference on Atmospheric and Oceanic Fluid Dynamics (Grotjahn and Immel, 2001). However, the figures here have not been reproduced elsewhere.

Figure 1(b) shows a maximum in the NP high central pressure over summer months of June through August. Monthly anomaly (MA) data were generated in order to remove any seasonal trend and to isolate variations between months. To calculate the MA for June 1979 (say), one averages all June data in the record used (1979–2004) then subtracts that average from the original June 1979 data; other months are handled analogously.

The MA data used include SLP, OLR, derived NCEP Reanalysis skin temperature (T<sub>skin</sub>), and CMAP precipitation rate (hereafter: P) as supplied by CDC. Several of the remote forcing mechanisms described above involve some type of divergent circulation where rising is presumed to occur at or near the site of the remote forcing. That rising motion is assumed to have associated precipitation. Hence, P (and OLR) data are used as a proxy for the remote forcing: higher P (lower OLR) is presumed to be associated with a stronger remote forcing mechanism. P data are not an ideal proxy since precipitation is influenced by factors other than vertical motion. Further, the reanalysis P data are determined by the reanalysis model instead of being directly assimilated. However, Kalnay *et al.* (1996) and Kistler *et al.* (2001) state that the reanalysis P data generally agree favorably with other published data. P data are used in the context of emphasizing relative differences, seeking consistency with other variables, and using monthly means. Measured OLR has better time

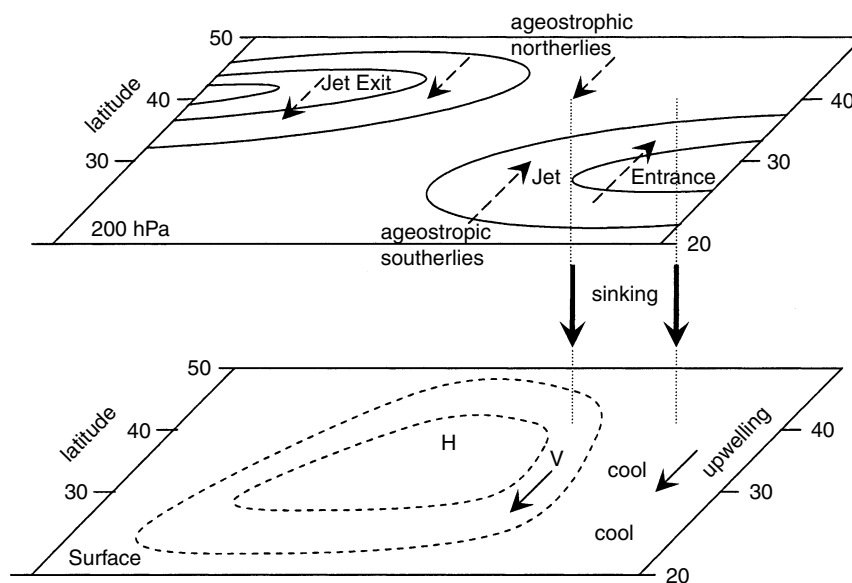


Figure 2. Schematic diagram showing upper level isotachs (solid lines), and upper level ageostrophic meridional velocities (dashed arrows) that create upper level convergence. Sinking (thick arrows) occurs on the east side of the high in the middle troposphere. Lower diagram shows SLP contours (dashed), low-level northerlies (thin solid arrows) that create upwelling and cool surface temperatures on east side of NP high.

and space coverage than P, but it has a latitudinal trend. Most of the results using P are duplicated using OLR.

For the monthly data, the analysis tools are of two types: composites and '1-point' correlations. The composites consist of isolating the 14 instances of highest central pressure in the NP high, the 14 instances of lowest central pressure, and examining the difference between averages of the two target groups. The statistical test is a simple (bootstrap) random resampling with replacement from the total sample (150 April–September monthly anomalies for 1979–2004). The 1-point correlations use rank correlations (Press *et al.*, 1992) because of the nature of the data. (For example, precipitation data in some regions of interest are zero during several of the months.) We further require the data to pass a 'Student's *t*' test. Plots often show a close correspondence between areas enclosed by the  $\geq 0.3$  correlation and areas passing the significance test at the 5% level.

For *daily* data, SLP, zonal and meridional upper level wind components, temperature, and interpolated OLR were obtained from the CDC websites. From these, divergent wind components and velocity potential (VP) were calculated. In Grotjahn (2004), VP was a more reliable field than daily P for the SP high. For the NP high, VP was not as useful an indicator of divergent circulations associated with midlatitude frontal cyclones than were divergent wind components. In this study, significant areas of VP are very large in scale. We find interpolated OLR to be more useful than P for daily data.

A Lanczos low-pass filter (Duchon, 1979) is applied to daily data. The filter effectively removes periods shorter than a 'cutoff'. Several cutoff values were tested in seeking a middle ground between having a cutoff long enough to reveal the tropical associations seen in the monthly mean data and short enough to allow a discussion of what leads what. A workable compromise turned out to be removal of periods less than either of 10 or 20 days, coupled with subsampling of the data at 4- or 5-day intervals. (Subsampling is used to improve greatly the relatively mutual independence of the data because consecutive days are not independent. Subsampling thereby improves the validity of the significance tests used.) Asymmetry with respect to zero lag of lead and lag correlations is used to establish cause and effect from lags that are less than the cutoff period.

One-point correlations and normalized regression plots were prepared for various variables that are thought to have a remote link to the NP high. Normalized regression plots may provide a better indicator of the magnitude of the remote association, and those results are emphasized here. The regression technique utilized in this paper is similar to the one described by Kiladis and Weickmann (1992), except that the statistical significance is determined by rejecting the null hypothesis that the regression coefficient is zero at the 1% level using a Student's *t* test. The secondary field, say OLR, is regressed against the SLP time series at the reference (or comparison) point. Once the linear regression model is obtained, the secondary field is reconstructed on the

basis of the model and a 'large' case SLP (sample mean, which is 0 in this case, plus 1 standard deviation) at the reference point. Furthermore, the reconstructed field is normalized by the local standard deviation at each grid point to attenuate the effect of local variance in the regression analysis. As a result, positive contours in the regressed field indicate positive correlation with SLP at the reference point, and vice versa.

The main statistical tests of daily data are one-point correlations and one-point regressions. These tests use data from June through August of the 25-year period (1 January 1979–31 December 2003). Lags and leads in either statistical test establish whether a remote process occurs before or after the corresponding change at the comparison or correlation point. Lead means the two-dimensional field occurs before the field at the comparison point. The filtering, subsampling, and the lag/lead are all done before retrieving the summer months from the entire data record. Therefore, the resulting parallel time series have no temporal discontinuity between years and the statistical tests are applied to the full parallel time series.

## RESULTS

### *Monthly mean data*

Maps in Figure 3 show correlations between a single 'correlation point' in SLP and a two-dimensional field – in this case precipitation rate P. Each correlation point is indicated by a circled asterisk. Shaded areas indicate significance  $>95\%$ . Dark shading means more P is associated with higher SLP at the correlation point and vice versa: less P with lower SLP. Light shading means lesser P occurs for higher SLP at the correlation point, and vice versa. H marks the NP high center location in the average of all June–August (JJA) periods in the total data. The months used are all JJA from 1979 through 2004. Both fields used to construct Figure 3 are anomaly fields (with the specific month's long-term mean removed). If total data are used the correlations are similar, though shaded areas become larger.

Higher correlation values tend to occur at remote spots, often on the same side of the high as the correlation point. Not surprisingly, precipitation tends to be suppressed in a region surrounding most correlation points. Exceptions are points to the southeast of the high center. Little of the P near Central America has significant correlation for correlation points on the center, north, west or southwest side of the high, contrary to the view that tropical convection east of the high forces the high. For Mexico and the southwestern US, P is less, not more, for higher SLP on the adjacent (southeast) side of the NP high. Higher SLP on the north side is associated with a storm track shift northwards over the Aleutian Islands. For higher SLP on the west side of the NP high there is more P over the western tropical Pacific, southeast Asian islands, and northern Indian Ocean. For the point at the center, the most prominent feature is a

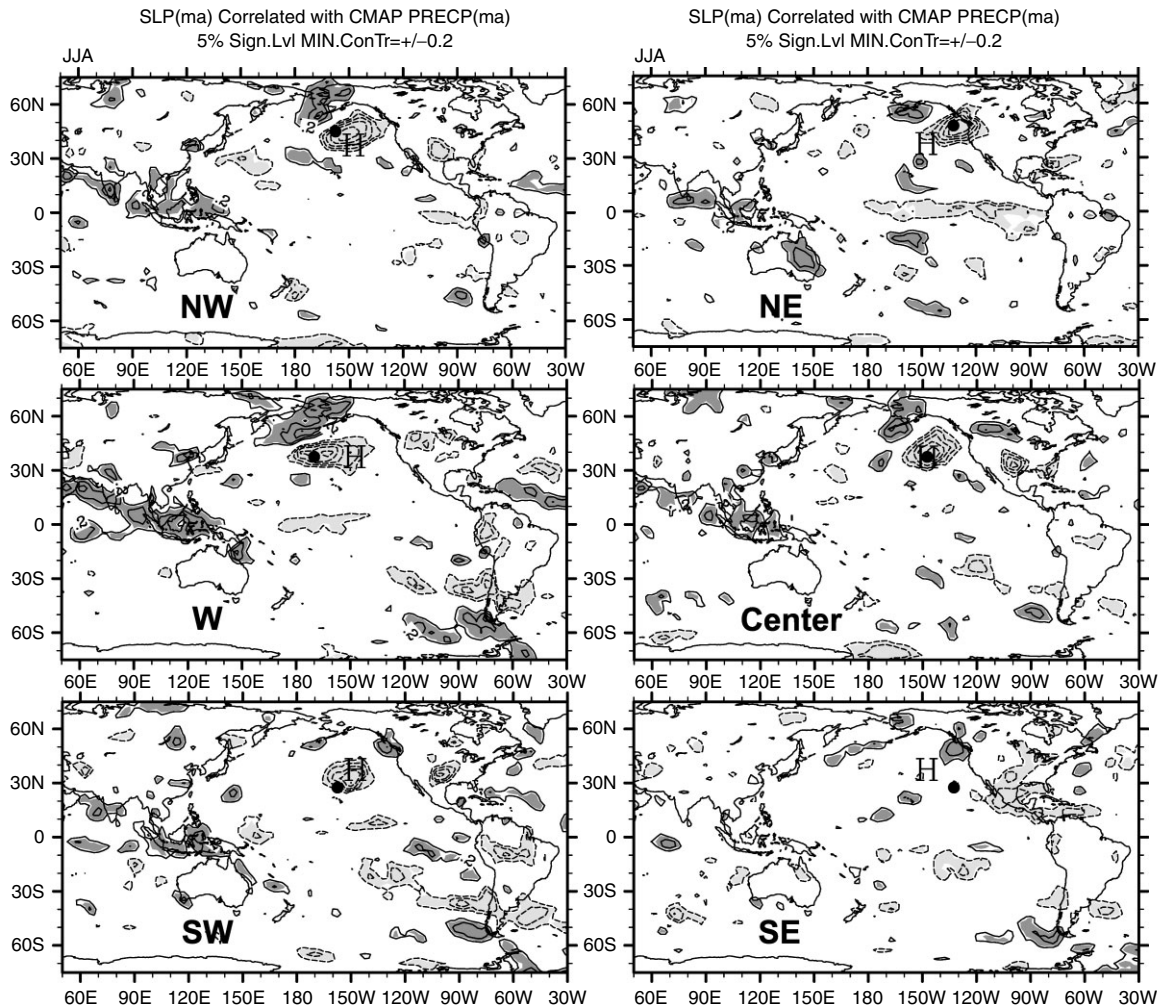


Figure 3. One-point correlation maps between the two-dimensional P (CMAP precipitation rate) field and SLP at the circled asterisk. Monthly anomalies for northern summer, JJA, from 1979–2004. Dark shaded areas denote highest 5% P with strongest SLP at the correlation point or lowest P with weakest SLP. Light shaded areas have high P with lower SLP or low P with higher SLP, again at the 5% level. Contour interval is every 0.1, with contours having magnitude less than 0.2 suppressed. The H denotes the climatological center of the high in the total field.

Directions of correlation points relative to the climatological center are indicated.

dipolar pattern suggestive of a shift of the midlatitude storm track precipitation, mainly upstream (west) of the high, but possibly downstream (east) as well. These data are potentially consistent with linking subtropical high strength to tropical convection to the south and west (a combination of ‘Hadley’ and ‘Walker’ circulations) and to a midlatitude storm track shift. Points west and south of the center also have dipolar association with P near the southern tip of South America. This Southern Hemisphere association suggests a common link rather than a direct connection. Evidence for a common link is found in Grotjahn (2004): a stronger South Pacific subtropical high (SP high) is associated with (a) South Pacific storm track shifted south, and (b) greater Indonesian-region P, though the stronger SP high preceded the stronger Indonesian P in lag/lead correlations of daily anomaly data. The proposed link to surface temperature is not addressed by these monthly mean correlations.

The correlation points shown sample the climatological center of the high and surroundings. Points diagonally

offset from the center are used because points southeast of the center have similar associations, but differ strongly from any other quadrant of the high. Since the high often has asymmetric shape with sharper gradient on the east side and broader gradient on the west side, an additional point is tested to the west in Figure 3. Other points were investigated, but are not shown here in order to keep the discussion compact. In general, the point to the NW of the center is representative of other points on the north side of the high. The point to the SE of the center is representative of the southeast quadrant. The point at the center is often similar to effects seen to the west and southwest of the center with these adjustments: (1) the further equatorward the point, the less the middle latitude association, (2) the further west the point, the greater the connection to the northern Indian Ocean and Indonesian region. These similarities are seen in Figure 3. Consequently, the most compact illustration of how the high is associated with remote processes is obtained by using the center, the southeast corner point, and the northwest corner point.

Composite results are shown in Figure 4 using MA data from April–September of 1979–2004. To construct the figure, 14 months having a stronger subtropical high in the central NP are averaged to form a target group, referred to as the strong high composite. Fourteen months having a weaker subtropical high are similarly grouped to form a weak high composite. The selection of the members of each composite was partly subjective. First, candidate months were identified starting with the strongest central pressure for the strong high cases (starting with the weakest for the weak high ensemble). A few (~20%) candidates were rejected owing to unusual shape of the high, such as having a multiple maxima, or a primary maxima far from the climatological mean position. Using monthly anomalies removes the seasonal trend, allowing the broad 6-month selection period. However, most of the composite members are from the core JJA period; few are from the fringes of the period (e.g. 2 of the 28 are from April). As a check, repeating the study using only JJA months (and smaller ensembles) produces qualitatively similar results; the main difference is that the larger ensemble has smoother contours.

Figure 4 shows the differences, strong minus weak composites for SLP and four other variables that are predicted by various theories to be related to subtropical high strength. The shaded areas denote differences that are unusually positive (dark) or negative (light shading). Significance is assessed by comparing the strong minus weak difference values to those from 600 differences between a pair of randomly selected 14-member groups.

The composite SLP differences of the (Figure 4(a)) strong target group minus weak NP high target group tend to be *higher* in these locations:

- (1) NP high (by design) but centered to the north of the mean position of the NP high (This conclusion applies to the SLP. It may interest some readers that the wind field is similarly shifted. For both total wind and monthly anomalies, the zonal wind component for strong high cases is shifted poleward compared to weak cases),
- (2) Subtropical south Pacific, consistent with results for the SP high (Grotjahn, 2004),
- (3) Northwest NP.

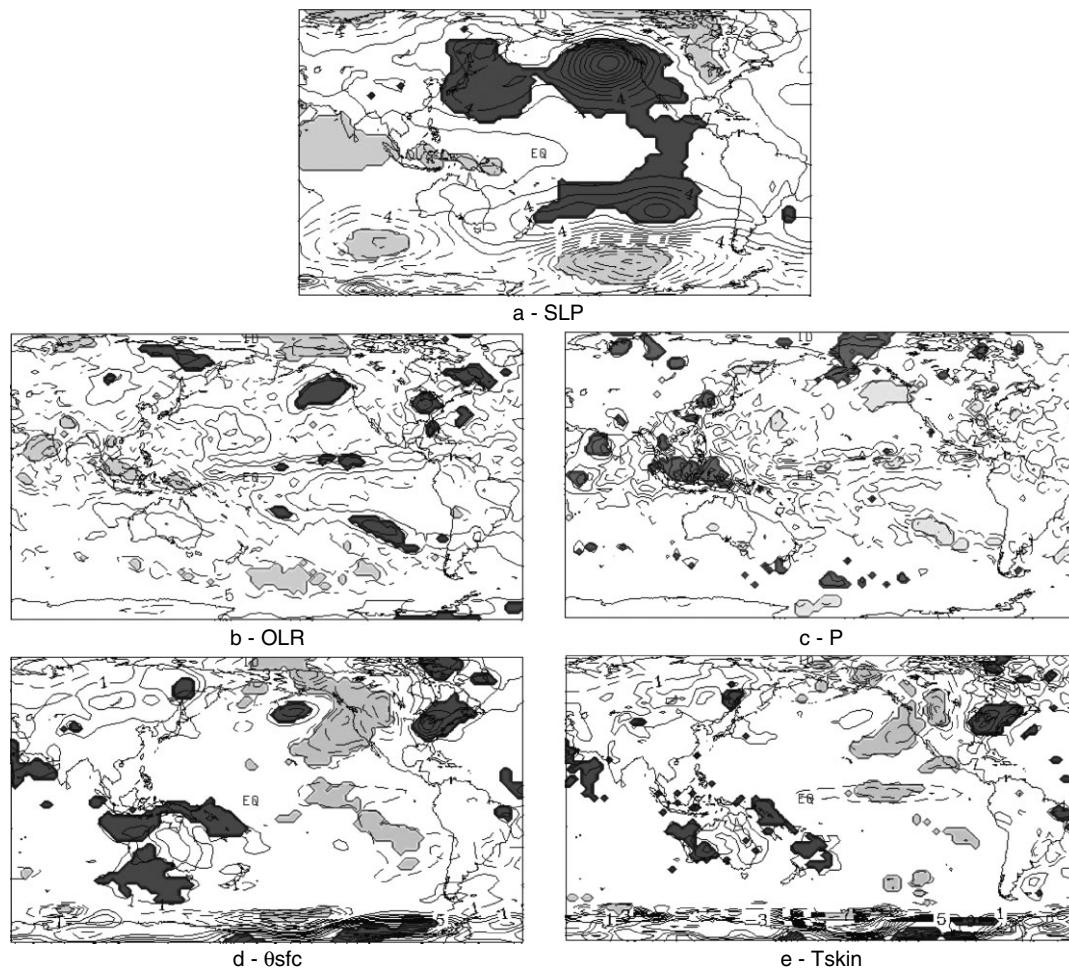


Figure 4. Monthly anomaly composite differences for a 28 member target sample (14 strong minus and 14 weak subtropical highs) drawn from April–September months in 1979–2004. Shaded areas denote highest 1% (dark) and lowest 1% (light) compared to randomly selected composites. (a) SLP, contour interval 2 hPa; (b) OLR, contour interval 10  $W/m^2$  with contours at odd integer multiples of 5; (c) P, with contours at odd integer values of mm/day; (d) surface potential temperature, contour interval 1 K; (e) surface skin temperature, contour interval 1 K. The zero contour has been suppressed in (d) and (e).

The strong minus weak NP high is also associated with lower SLP in these locations:

- (1) Central Canada and parts of the Arctic Ocean,
- (2) Tropical Indian Ocean,
- (3) Islands of Indonesia extending across the Coral Sea,
- (4) Southern midlatitude Indian Ocean,
- (5) Southern midlatitude Pacific Ocean.

Owing to their lesser extent and/or magnitude, two other significant areas are not emphasized: higher SLP over South Africa (not shown) and lower SLP off Argentina. These patterns show up in the stronger NP high target sample and, with opposite sign, for the weak target sample. The low centers in Figure 4(a) are not sensitive to the size of the composite target group or number of random groups. The challenge is to explain these features.

To explain the SLP differences of Figure 4(a), it is useful to examine other fields that are expected to be associated with SLP. Associated large SLP differences seen far away in the southern midlatitudes may suggest a common cause, such as a response to greater tropical P and lower OLR (Figure 4(c) and (b), respectively) near the Arabian Sea and across Indonesia to New Caledonia. Such anomalous convection could strengthen the midlatitude subtropical jet in both Northern and Southern Hemispheres (e.g. Sardeshmukh and Hoskins, 1988), potentially affecting the midlatitude cyclones of both hemispheres. However, the monthly averaging precludes establishing cause and effect. Neither the OLR nor the P over Central America or southwestern North America is associated with the SLP difference. One might have expected an association from the Rossby wave mechanism (e.g. Rodwell and Hoskins, 2001).

The association with convection from Indonesia eastward to the tropical eastern Pacific suggests that one might expect a similar association with SST. Figure 4(e) tests that association with SST by compositing surface skin temperature. The strong minus weak SLP difference is associated with significantly lower skin temperatures (by several degrees) over the tropical central and eastern Pacific and covering the eastern and much of the southern side of the NP high. Figure 4(e) also shows association with warmer oceanic skin temperatures: roughly in a band extending southeastward from New Caledonia to an area northeast of New Zealand. A region of the Arabian Sea is also warmer. Colder skin temperatures occur over the central and eastern tropical Pacific. Since such cooler waters would suppress or shift intertropical convergence zone (ICZ) convection southwards, the pattern seems consistent with the 1-point correlations (Figure 3), especially for the NE point; a correlation point on the north side is centered where the SLP composites have largest difference (Figure 4(a)). Over land, the colder skin temperatures on the east side of the high carry across into central Canada while skin temperatures warmer by several degrees are found further east over the Great Lakes region. The dipolar pattern of skin temperature

over the Canada–US border region is seemingly consistent with advection around the anomalous SLP trough seen in Figure 4(a).

Local forcing of the high by surface potential temperature ( $\theta_{\text{sfc}}$ ) over the western US and adjacent waters is investigated in Figure 4(d). The composite difference pattern for  $\theta_{\text{sfc}}$  is largely similar to the skin temperature results discussed above. Like the skin temperature results, the surface potential temperature results are consistent with local PV thinking of cold water leading to higher SLP. Cooler than normal surface temperatures preponderate over the western side of the continent instead of the hot temperatures envisioned by the PV dipole mechanism, though there are warmer than usual surface temperatures much further east over the continent. The  $\theta_{\text{sfc}}$  difference pattern seems to be at least partly explained by advection around the anomalously higher pressure of the stronger highs. One difference from the skin temperature results is over the region of Indonesia to Papua New Guinea. Lower SLP there (Figure 4(a)) could explain the higher  $\theta_{\text{sfc}}$ , though this could also be a matter of the threshold (1% significance) chosen to initiate the shading in significant skin temperature correlation.

A near-surface potential temperature couplet (cool ocean over the entire high, warm over the Rockies and eastern US) is shown in Miyasaka and Nakamura (2005), model results generated from lower tropospheric diabatic heating. However, this is only partially seen in our observed composites. While much (except the NW part) of the high is associated with cool surface theta and the eastern US is warm, the Rockies are cool, both in temperature and potential temperature (Figure 4(d), and (e)).

Monthly data conclusions:

- (1) Correlations show that the dominant remote association tends to be that on the corresponding side of the high. More tropical P over Borneo and adjacent waters and less P over Mexico are linked to higher SLP on the south side of the NP high. A poleward shift of midlatitude storm track and more P to the south of the high are associated with higher SLP on the north side of the NP high. For higher SLP on the tropical side, the midlatitude storm track is shifted south. Shift of the midlatitude P is inferred from a dipole pattern because the climatological axis of maximum P lies between the positive and negative of the dipole in the NP.
- (2) The stronger NP highs are those that are poleward of the climatological position, a result also found for the SP high.
- (3) Composite differences of strong minus weak NP highs have three main regions of higher SLP and five main regions of lower SLP.
- (4) Associations are found for quantities far away from the NP high, suggesting some associations may have a common cause rather than a direct link.
- (5) Evidence consistent with proposed tropical and midlatitude forcing mechanisms is found, including

regional surface potential temperature, but cause and effect is not yet determined.

#### Daily data

Understanding the sequence of events for the structures in the SLP and associated fields (e.g. Figure 4) is crucial for ruling out or ruling in different theories that have been proposed. Daily data have sufficient time resolution to allow the timing of events to be deduced. When the raw data are used, all associations are swamped by the local higher frequency frontal cyclones. In order to identify and track other remote associations, it proves necessary to filter out frequencies higher than a cutoff period.

*Autocorrelations/autoregressions.* A Fourier transform of the autocorrelation function was calculated for each year, then the functions were averaged. The magnitude of that transform is sometimes called the power spectra (e.g. von Storch and Zwiers, 1999), though some authors (e.g. Wheeler and Hendon, 2004) call the power spectrum the square of the transform multiplied by the frequency. The power spectrum discussed here is the transform squared multiplied by frequency. The power spectrum for various midlatitude points has peak amplitude around 12–25 days. For other points (at the latitude of the NP high peak value as well as on the tropical side of the NP high) there is a second maximum in the range of 50–30 days, this period, along with the linkage seen with Indonesian-region low pressure, is suggestive of a connection to the Madden Julian Oscillation (MJO). The power spectra reveal a relative minimum between the 2–3-week period and the 50–30-day period at most grid points around the NP high. To reduce the frontal cyclone track influence and enhance tropical associations, a low-pass filter having a cutoff period between 30 and 20 days is useful. Choosing a cutoff at the low end of this range assists with determining whether an associated phenomenon leads or lags the NP high SLP property. Hence, a 20-day cutoff filter is judged sufficient to remove most of the midlatitude frontal cyclone activity and help isolate the tropical associations.

Filtered, normalized, autoregression curves for global SLP and SLP at a comparison point are shown in Figure 5 at 4 days lead and 4 days lag. (Lead means the two-dimensional field occurs before the field at the comparison point. Vice versa for lag.) To emphasize what tends to lead what, the zero lag has been omitted and the discussion focuses on the asymmetry of the significant regressions. The comparison point at the center of the NP high appears to be led by higher SLP just east of Japan and lower SLP over the Indonesian archipelago and over central Canada. Higher SLP at the comparison point appears followed by lower SLP over parts of the Indian Ocean and possibly higher SLP over Central America. The pattern across the middle latitudes is somewhat like a wave train. The stronger high being preceded by low pressure over central Canada implies enhanced northerlies east of the NP high, which may amplify colder

low-level temperatures on that side of the high. While the magnitudes of the SLP changes are small in the tropics, they exceed 20% of a standard deviation in that region.

Autocorrelations for SLP using a correlation point at the location of the climatological maximum in SLP and for other midlatitude points also find significant correlations appearing as a midlatitude wavetrain. A similar wavetrain was found in Southern Hemisphere midlatitudes for the SP high (Grotjahn, 2004). For low-pass filtered SLP using a 7-day cutoff period, longer waves appear in the autocorrelation having wavelength of 60–80 degrees longitude (i.e. zonal wavenumber 4–6). At zero lag, there is negative autocorrelation ( $>0.3$ ) over central North America. While 4 days earlier, there was significant positive correlation ( $>0.3$ ) just east of Japan (centered 60 degrees west of the correlation point). Though there are large coherent areas passing a 1% significance test in the tropical Indian Ocean, the correlations are small ( $<0.2$ ).

For a representative point on the northwest side of the NP high, the autoregression pattern is similar to that found for the central point, except that the indication of what leads what is perhaps more clear. The higher SLP east of Japan and the lower SLP over central Canada clearly lead the comparison point. The area of lower SLP in the equatorial Indian Ocean, moving across into the western equatorial Pacific, more clearly leads the higher SLP at the NW comparison point. The higher SLP over Central America that follows the higher SLP at the comparison point is more evident for the NW point than for the central point. The way in which the autoregressions vary from the NW to the central point may be extrapolated to deduce the pattern for a point on the southwest (not shown) side of the NP high: even less connection to the leading Northern Hemisphere 'wave train' and lowered SLP in the Indian Ocean, greater association to SLP in the east Pacific tropics and southern midlatitudes.

For a correlation point due south of the high center, the autocorrelation (not shown) at zero lag has significant correlation ( $>0.2$ ) over the entire tropical Pacific, including south of the Equator. Autoregressions (not shown) for points on the S or SW side of the NP high also find this. This result is consistent with SP high autocorrelation (for the opposite time of year). Autocorrelations and autoregressions show stronger SLP in the equatorial Pacific, and a southward shift of the Southern Hemisphere storm track southwest of Chile follows higher values at a point south or southwest of the NP high. The shift in the southern midlatitudes SLP is more prominent 8 days prior and seems consistent with the composite results (Figure 4(a)). There is little correlation with SLP in Northern Hemisphere middle latitudes, at zero lag or later times. However, autoregressions have lower SLP over Canada lagging the comparison point.

For an autoregression comparison point or for a correlation point on the southeast side of the NP high, the significant autoregression and autocorrelation patterns are strong and extensive in the tropics. A similar

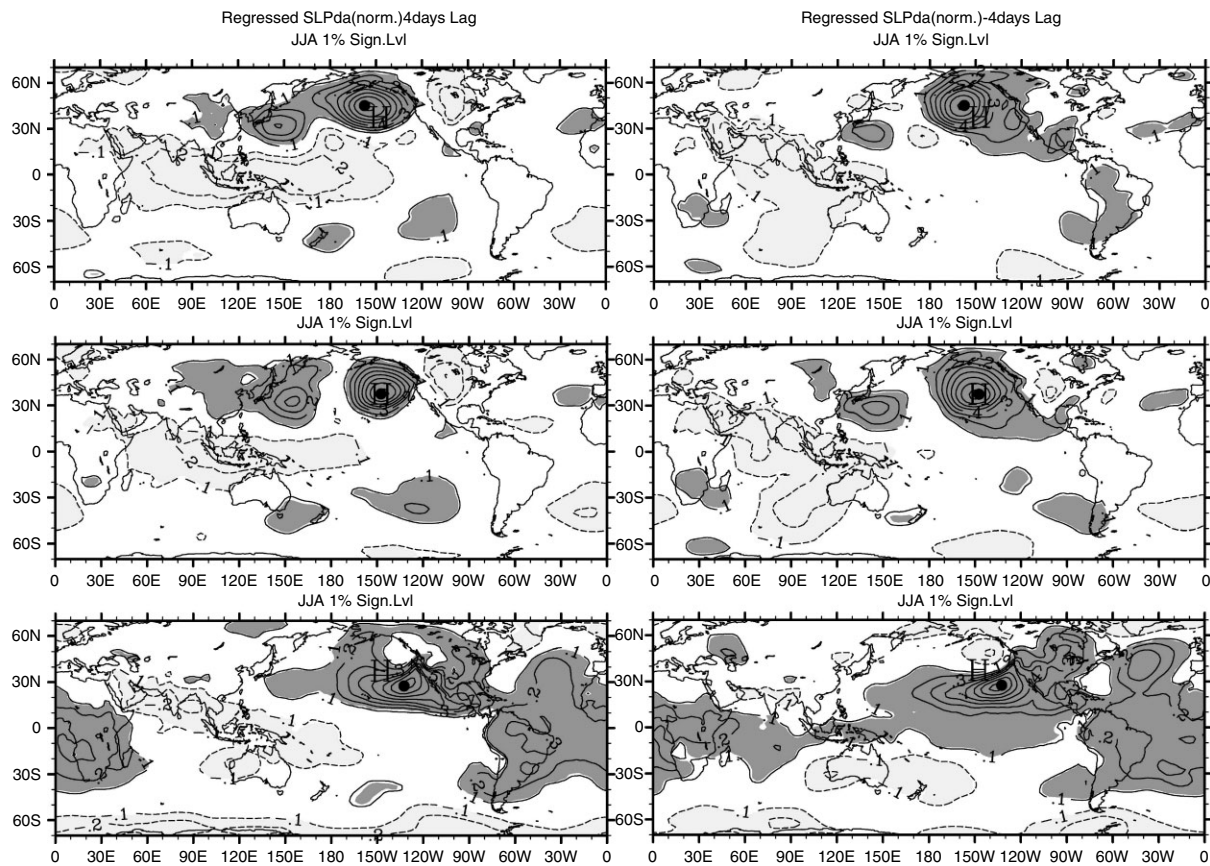


Figure 5. Filtered, normalized SLP autoregressions for three points: at a point in the northwest side of the high (top row), at the 'center' of the NP high where SLP has climatological maximum value, (middle row), and a point on the southeast side (bottom row). The left column is where the two-dimensional (2D) field occurs 4 days before the values at the correlation point. For the right column, the 2D field occurs 4 days after the correlation point. Solid contours (in dark shading) mean correlation  $\geq 0.1$ , with interval 0.1. Dashed contours (in light shading) for negative correlation  $\leq -0.1$ . Daily anomaly data for JJA during 1979–2003 are low-pass filtered to remove periods of 20 days or less (20 day cutoff) and then subsampled every 4 days prior to the regression. Regressed values are based on one standard deviation at the comparison point. The 2D values are normalized relative to the local standard deviation. All shading indicates significance at the 1% level.

phenomenon occurs in 1-point correlations (e.g. using 7-day cutoff, not shown). Judging by how the regressions change from lead to lag, lower SLP over a swath across the northern Indian Ocean into the western equatorial Pacific as well as higher pressure over Central America clearly lead higher SLP at the comparison point. Other regions of higher SLP are Amazonia and southern Africa, which appear to lead the higher SLP at the comparison point, though it is difficult to understand how these regions are associated with the NP high directly. For autocorrelations, higher SLP on the southeast side of the high is preceded by lower SLP in the western tropical Pacific 8 days before. At shorter lags higher SLP at this point is associated with higher pressure through most of Mexico, Central America, northern South America, and the tropical Atlantic. Curiously, this point has almost no significant correlation with points at or poleward of the NP high in the North Pacific, except for negative correlation (lowered SLP) off Canada's Pacific coast. The correlations 8 days after higher SLP at the correlation point (not shown) are all  $< 0.2$ .

*OLR correlations/regressions.* Figure 6 shows normalized regressions of the 2D filtered daily anomaly OLR

field and corresponding SLP at the same comparison points highlighted in the previous figure. For a point on the northwest side, a wave train shows up similar to that seen for the autoregressions. Higher OLR near the reference point and just east of Japan appears to lead the change at the reference point. Higher OLR over the central and eastern US and lower OLR south of the NP high appear to follow the comparison point. It is unclear whether lower OLR over Canada and the northern Indian Ocean follow or lead the reference point. For a point at the NP high center, elements of the midlatitude wave train appear similar to that described for the NW comparison point: higher OLR leading east of Japan, following over eastern North America; lower OLR leading over Canada and following to the south of the NP high. The association to OLR over the northern Indian Ocean and Indonesia is not as prominent as for SLP. For the central point of the NP high, the area of significant lowered OLR migrates northward as time proceeds from lead to lag. The regressions are small, ranging from  $-0.1$  to  $-0.2$  for 4 days lead and  $-0.2$  to  $-0.3$  for 4 days lag. There is a tiny area in a part of the North American monsoon where negative OLR precedes the higher central SLP. This tiny area would be consistent with the

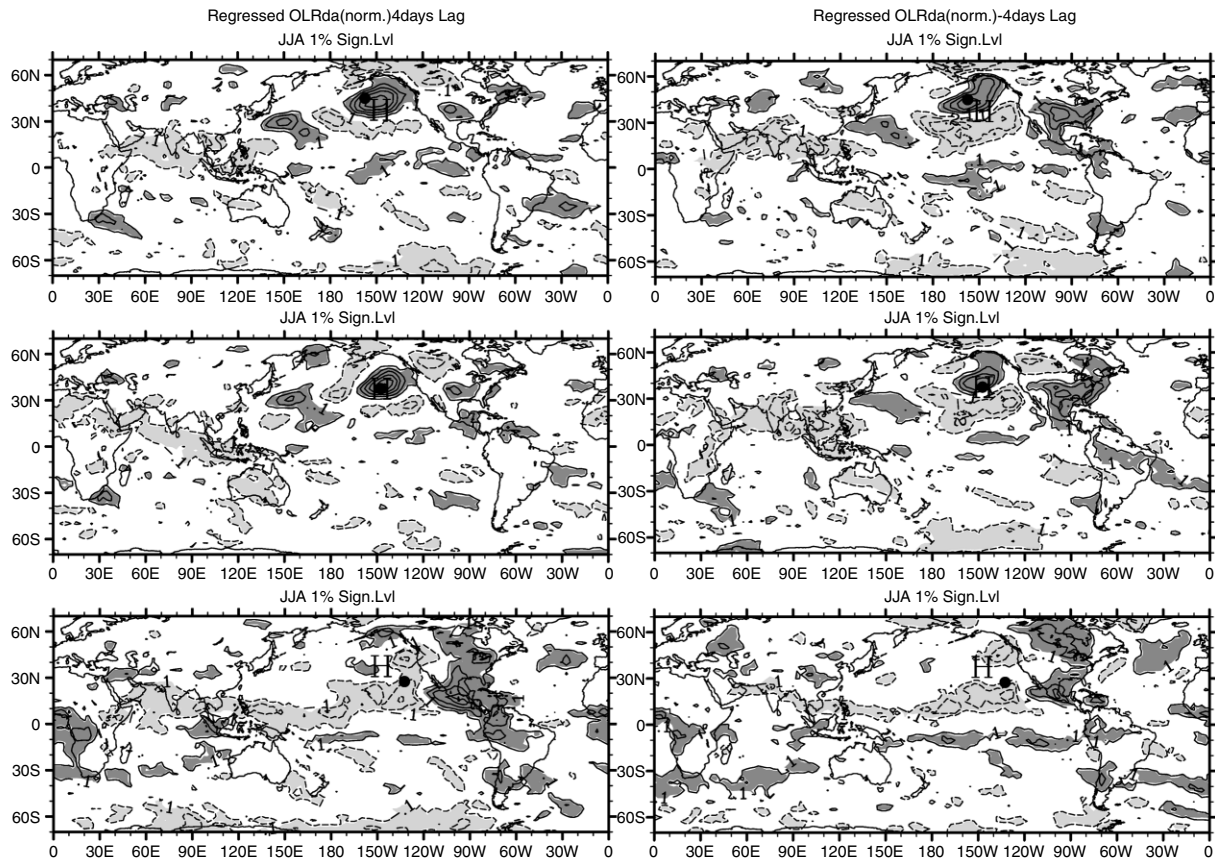


Figure 6. Similar to Figure 5 except normalized comparison of SLP at the comparison point against 2D outgoing longwave radiation (OLR). Solid contours mean that higher SLP at the comparison point is associated with higher OLR, and vice versa. Dashed contours are negative regression. Subsampled (4 day) daily low-pass filtered (20-day cutoff) anomaly fields from JJA during 1979–2003. Contour interval of 0.1 starting with 0.1.

Rossby wave mechanism, but it is unimpressive (normalized regressions barely greater than 0.1) compared with the other associations seen here; furthermore, much of Central America has higher OLR preceding the stronger SLP at the NP high center.

1-point correlations (not shown) using the same subsampled, filtered OLR and SLP tell a similar story. When 8 day lead/lag correlations (not shown) are tested, there is relatively little significant OLR 8 days prior; just higher OLR in the area of the NP high. In contrast, 8 days after higher NP high SLP, there are broad areas of significant OLR correlation. Higher OLR over southeastern North America and Central America and the area of lowered OLR on the south side of the NP high remain prominent as they were in lagged regressions. Also, similar to the regressions, the apparent northward migration of lower OLR to a swath across India and southeast Asia at 8 days lag is also present in correlations using the central point. Positive correlation is found at lead times just east of Japan, similar to regressions. Composite data (Figure 4(b)) contain several of the features seen for the regressed OLR at the central point: significant high OLR on the north side of the high, over eastern North America, near the central Pacific section of the ICZ, and significant lower OLR over Indonesia and the Arabian Sea. Composite data have negative OLR on the south side of

the high, similar to the regressed data and correlations, but it does not pass the significance threshold for the composites.

For a point on the southeast side, similar to autoregressions, there are large areas of significant correlation, particularly in the tropics. Higher OLR over Central America and lower OLR over the west Pacific seem to precede the higher SLP at the comparison point. There is a dipolar structure across most of the Pacific that straddles the ICZ. To the extent that lowered OLR suggests increased cloudiness and precipitation, then this dipole suggests that higher SLP at the reference point SE of the NP high is associated with a northward shift of the ICZ. For other points on the south and southwest side of the NP high, the dipole in the regressed OLR field is present, but not so prominent. In correlation data using longer leads and lags, there seems to be a preference for the apparent ICZ shift to follow the reference point.

In terms of our theoretical guidance, it seems that excess precipitation (using OLR as proxy data) over Central America and Mexico does not drive subsequent higher pressures over the NP high. Indeed, the opposite seems the case. As with the autocorrelations, this result means *suppressed* convection over Central America precedes stronger SLP on the southeastern quadrant of the NP high. At times after the SLP peaks at a southeastern

correlation point, the OLR over Central America has no significant correlation with that SLP. Elsewhere, OLR is less to the southwest of the correlation point and greater over a few small regions (e.g. central Canada) 8 days after the SLP at the southeast correlation point.

*Divergent circulations.* One-point correlations for 200 hPa level VP were useful for interpreting remote associations with the SP high. However, VP data seem less useful for the NP high investigation because the VP regressions and correlations have very large scale (mainly global zonal wavenumber 1 and little meridional variation from pole to pole). Regressed VP fields (not shown) have a slow eastward migration as time proceeds from lead to lag. Four days prior (lead) there is positive VP (normalized regression  $>0.4$ ) on the northeast side of the NP high, along with negative VP ( $-0.2$  to  $-0.3$ ) over Asia and much of the Indian Ocean when the reference point is at the NP high center. The pattern of regressed VP at 4 days lag is similar, except that it is shifted east, and with the Asian region more strongly negative and the area just northeast of the high reduced by half. The regression pattern seen for the central point recurs for points west or north of the center. For a comparison point on the southeast side of the high, higher SLP is preceded by stronger VP over the Caribbean, eastern North America, and adjacent Atlantic. Correlations between SLP and upper level

divergent wind components (not shown) show a similar result. At 200 hPa, divergent meridional northerly winds fill the NE quadrant above the NP high while weaker southerlies are found to the southeast of the reference point. The pattern is consistent with schematic Figure 2. The correlation patterns have dipolar structure centered to the northeast of the correlation point by 5–10 degrees latitude and longitude. The dipolar structure in both components shows enhanced upper level convergence northeast of the correlation point, which appears to precede stronger SLP by few days. There was no notable correlation with upper level tropical divergent wind components when using a 7-day cutoff low-pass filter.

*Temperature fields.* Daily surface potential temperatures ( $\theta_{sfc}$ ) were regressed against SLP at various points surrounding the NP high. As elsewhere, the data were low-pass filtered (20-day cutoff) and subsampled. Normalized regressions are plotted in Figure 7. For a reference point northwest of the center, cooler potential temperatures prevail on the north, east, and south sides of the NP high, these negative regressions are larger at 4 days lag and so appear to follow increased SLP at the northwest reference point. These negative (cooler) regressed  $\theta_{sfc}$  values also seem to rotate clockwise from the northeast to the southeast and south side of the NP

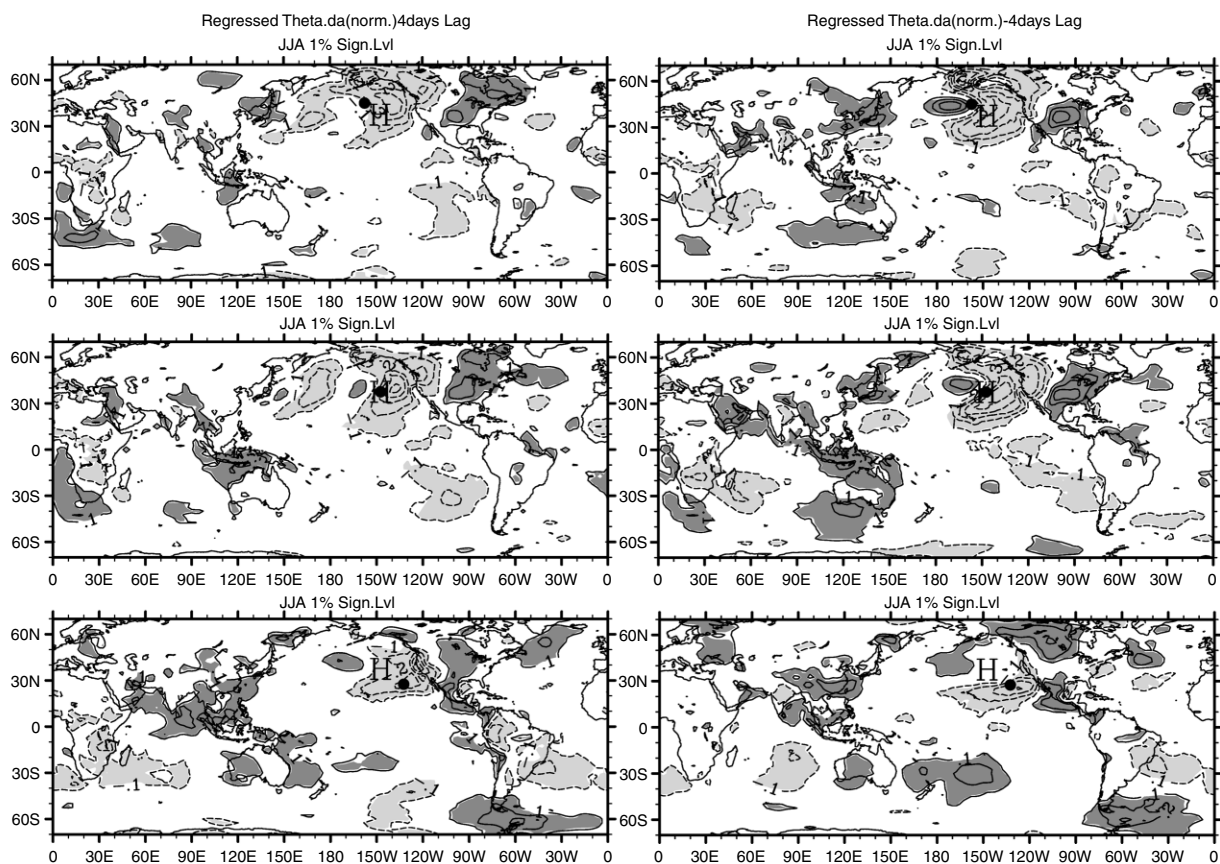


Figure 7. Similar to Figure 5, except normalized 2D surface potential temperature ( $\theta_{sfc}$ ) is regressed with SLP at various points. Solid contours mean higher SLP at the comparison point is associated with higher  $\theta_{sfc}$  and vice versa. Dashed contours are negative regression. Subsampled (4 day) daily low-pass filtered (20-day cutoff) anomaly fields from JJA during 1979–2003. Contour interval of 0.1 starting with 0.1.

high as time progresses from lead to lag. Surface potential temperature may be influenced by pressure changes as well as temperature changes. Daily skin temperatures are examined to identify whether SLP increase (say) leads to surface potential temperature fall. When skin temperature is regressed instead of  $\theta_{\text{sfc}}$ , regressed cooler skin temperatures have weak significance over the ocean, and only in the 4-day lag data. In contrast, the cooler regressed  $\theta_{\text{sfc}}$  values over western Canada are well-matched by cooler skin temperatures; in both cases there is a slight preference for larger regression at 4 day lag. The skin temperature and  $\theta_{\text{sfc}}$  data seem consistent with advection around the high of cooler temperatures from the north and with that advection being amplified as the high amplifies. Advection may also explain the preference for warmer temperatures over eastern North America to lag behind the SLP change at the reference point. A SLP trough over central Canada appears in autoregression (Figure 5), composite (Figure 4(a)), and autocorrelation (not shown) results, with a preference for that trough to lead the SLP changes at the NP high.

For a reference point at the NP high center, regressed  $\theta_{\text{sfc}}$  values are largely similar to those described for a point NW of the high. Cooler temperatures develop south and east of the high after SLP has increased at the central point. Cooler  $\theta_{\text{sfc}}$  values in the Bering Sea (and south of it) are not replicated in regressed skin temperatures. The center of the high has larger tropical areas of significance, particularly in the SP high region, Indonesia, and Indian Ocean. However, while these areas have a similar sign in regressed values of skin temperature, these regions are not significant in skin temperature.

Like the regressions, correlations between SLP and daily surface potential temperatures ( $\theta_{\text{sfc}}$ ) have a strong signal primarily in the middle latitudes. Generally, the correlation patterns are similar to the regressed  $\theta_{\text{sfc}}$  values shown. When a 7-day cutoff is used the only significant signal seen is over the midlatitudes of the NP and North America. When a 20-day cutoff is used the midlatitude signal has even greater correlation while other areas of the tropics and even Southern Hemisphere have a significant correlation greater than 0.2. Strengthening the NP high near where it has largest magnitude climatologically, where it has largest composite difference, and on the west side of the high are all associated with decreased surface potential temperature values at and to the immediate east of the correlation point and increased values much further east over North America, and the warmer surface potential temperatures over North America clearly follow, by several days, the SLP changes over the NP.

The connections to tropical phenomena require a longer cutoff period than 7 days. Using a 20-day cutoff finds a correlation between higher surface potential temperature in the area of Indonesia and New Guinea and stronger SLP on the south and southwest side of the NP high. The correlations are small (generally around 0.2). Among other weak preferences in the 20-day cutoff data, a weak preference is seen for warmer temperatures in the tropical Atlantic possibly leading higher SLP. The

longer cutoff period obscures the preference for warmer temperatures over North America and off Newfoundland to follow the SLP change for this point.

Regressed  $\theta_{\text{sfc}}$  (Figure 7) and skin temperatures for a reference point on the southeast side of the high have these similarities to other reference points. Cooler temperatures over the west coast of North America are still present, but less prominent than other correlation points shown. Warmer temperatures over northern Canada seem to follow the higher SLP on the SE side of the NP high, which have large significant areas in the tropics and Southern Hemisphere. Cooler  $\theta_{\text{sfc}}$  and skin temperatures prevail near the reference point and are stronger after the higher SLP at the reference point. Different from other reference points are higher regressed  $\theta_{\text{sfc}}$  and skin temperatures over most of Central America and far northern Canada, which follow the higher SLP. Higher  $\theta_{\text{sfc}}$  and skin temperatures appear to migrate northward into southern China as time progresses from lead to lag.

The regression and correlation results support a local relationship between higher SLP and cooler surface temperatures. These results do not support the notion that a couplet of heating and cooling drives the stronger high over timescales of a week or more. In terms of our theoretical guidance, warmer inland temperatures do not drive higher SLP for the NP high. Indeed, the opposite seems the case in that cooler inland temperatures are associated with higher SLP on the eastern side of the NP high. Furthermore, higher temperatures associated with the NP high develop over the central and eastern US and Canada after the occurrence of higher SLP over the NP high.

It should also be noted that the sinking over the region east of the NP high would imply adiabatic warming of the air there. This sinking contributes strongly to the high temperatures observed over the Sonoran desert. To obtain cool surface temperatures over the NP high, it requires some separation (to the west) of the sinking and is presumably augmented by surface heat fluxes from cool (upwelled) ocean waters.

*Climate indices.* At its heart, the El Niño–Southern Oscillation (ENSO) has changes in equatorial Pacific SST. The associations between NP high SLP and surface thermal variables raise the question of how the NP high would be linked to ENSO. The ENSO connection was explored in Grotjahn (2004) (Figure 11 in Grotjahn, 2004) for December, January, February (DJF) monthly data, with focus primarily on the SP high. Correlations between the Niño 3 + 4 mid Pacific SST and SLP on the southeast side of the NP high are in magnitudes that exceed 0.5 (cooler SST with higher SLP and vice versa). The correlation with the Southern Oscillation index (SOI) is comparable ( $>0.5$  for the southeast side of the NP high). These peaks are rather close to the climatological location of the NP high during winter (Figure 8, top row). However, in summer the SLP of the NP high has much less correlation to ENSO

(Figure 8, bottom row). In summer, the significant areas of monthly mean data do not extend north far enough to reach the center of the NP high or any of the surrounding points discussed above. Hence, ENSO has little association to the NP high in monthly data during summer.

SLP at many of the points surrounding the NP high have large power spectral peaks in the 30–50-day period. In addition, the composite data, the regressions, and the one-point correlations suggest associations with P and OLR over the tropical western Pacific extending westward across into the Indian Ocean. The MJO helps organize the precipitation in that region and has a period similar to the SLP spectral peaks. Hence, it is worthwhile considering what association the NP high has to the MJO. Wheeler and Hendon (2004) developed daily values of two empirical orthogonal function (EOF) patterns that help identify different stages of the MJO in observational data. Their indices are applied here during NH summer months, though it should be recognized that the indices are larger in the NH winter months. The indices track the eastward progression of MJO convection. To relate these indices to SLP, the following progression is to be noted: negative eof2 (enhanced convection in Indian Ocean), then positive eof1 (enhanced convection over and slightly east of Indonesia, suppressed convection over and east of South America), then positive eof2 (convection over central Pacific with suppression

over Indonesia), then negative eof1 (enhanced convection over and east of South America, suppressed convection over Indonesia). Correlating SLP data with these MJO indices during June–August reveals significant but small (0.2–0.3) correlations (Figure 9). SLP is higher over the tropical and subtropical NP for eof1 positive, with a slight preference for 16–24 days prior to the peak in eof1. This correlation is consistent with negative eof2 occurring earlier by about that amount of time and with the eof1 autocorrelation negative minimum (Figure 12 in Wheeler and Hendon, 2004). A similar, but much smaller, portion of the same region has lower SLP prior to and during the positive eof2 (when correlated with eof2). Correlations assume symmetric response for negative and positive indices. The SLP changes in the tropical and subtropical NP are partly consistent with the enhancement or suppression of the ICZ convection as MJO-enhancement of convection migrates east. The asymmetry of the response suggests that the SLP may be driving stronger northeast trades (recall Figure 5) that subsequently enhance the Indonesia–New Caledonia region precipitation. The MJO indices do not have a notable correlation with middle latitudes, except between eof1 and a small area in the Tasman Sea. Correlations between SLP and eof2 do not have notable correlations in middle latitudes. The most prominent correlation, not yet mentioned, is over tropical

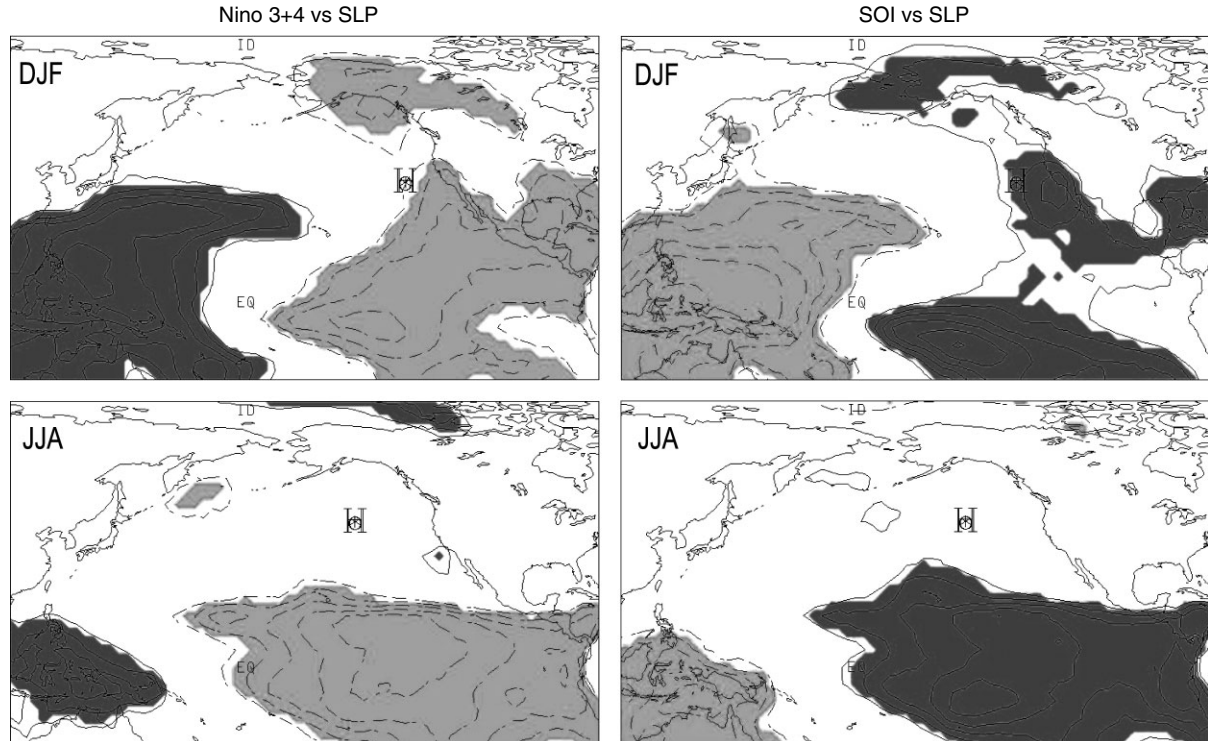


Figure 8. Correlation between SLP and Pacific SST anomaly Niño 3.4 (left column) and between SLP and SOI (right column). Top row is December–February data and bottom row is June–August data: monthly anomalies from 1979–2003. Shading indicates that the correlation at the grid point passes a significance test at the 1% level. Contours start with magnitude 0.3 and have 0.1 interval; dashed contours (with light shading) indicate negative values. The **H** symbol marks the climatological location of the NP high. The top row extends the geographic region shown in Grotjahn (2004). Both indices have a significant correlation near the climatological high center in winter but little correlation during summer.

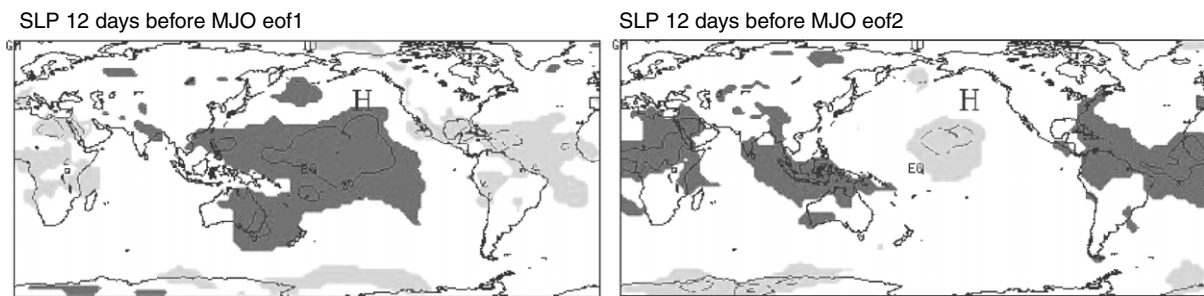


Figure 9. Correlations between 2D SLP and two MJO indices (see text). Significant SLP changes occurring 12 days before an MJO index value is plotted. Summertime daily anomaly data for 1979–2003 used. Contour interval of 0.2.

South America and the adjacent tropical and subtropical Atlantic; higher SLP there precedes positive eof2 by 16–32 days and reappears 8 days after the peak positive eof2.

### SUMMARY AND CONCLUSIONS

The spatial pattern of the correlations of daily data and power spectra reveal that NP high variations are dominated by middle latitude frontal cyclones. Power spectra also find peaks in low frequencies that include tropical as well as middle latitude circulations. The lower frequency correlation patterns differ from the high frequency patterns, primarily because high frequency patterns do not have much significance in the tropics. The low frequency patterns are emphasized by monthly mean data.

Composites of monthly mean data were made and associated with other fields that are thought to be related to NP high properties. Composite difference fields of strong minus weak NP highs show higher SLP: at the high (by design, though the largest difference is north of the mean center) and to the west (near Japan) and in the subtropical SP. Grotjahn (2004) found the stronger SP high to be similarly poleward of the climatological mean position by 5–10 degrees latitude. Grotjahn (2004) and others have found the subtropical SLP of the Pacific correlated between hemispheres. The composite differences find lower SLP: over central Canada, in a band from the Indian Ocean across to New Caledonia, and in the Southern Hemisphere midlatitude storm tracks. The composite SLP difference in that tropical band lies between 2 and 4 hPa. The Southern Hemisphere middle latitudes have a dipole pattern: higher at the SP high and lower in the storm track, implying an intensification of both, perhaps due to a narrowing of the meridional extent of the storm track. Corresponding composite differences find more precipitation rate  $P$  (and less OLR) in a band from the South China Sea across to New Caledonia, with less  $P$  over both the NP high and the west side of the SP high. A dipole in  $P$  over Alaska and the NP suggests a poleward shift of the NP storm track. The association of lower  $P$  on the south and west side of the SP high is consistent with the SLP correlation and possibly with a poleward shift of the southern Pacific

midlatitude storm track. There is some indication of a southward shift of the Pacific ICZ with increased OLR on the north side and small dipolar  $P$  changes. Colder skin and surface potential temperatures occur south and east of the high, with warmer temperatures further east over eastern North America and in a small area northwest of the high center. The small area of warmer potential temperature northwest of the high center might be ascribed to advection by southerlies on the west side of the NP high (skin temperatures are warmer there too, but do not pass the 1% significance test). Corresponding surface potential temperature differences show warming in a band north of Australia, which is partly due to lowered SLP in the region since the difference is less apparent in skin temperature.

Monthly mean data of SLP at selected points around the NP high were correlated with the two-dimensional field of  $P$ . Such correlations show that more tropical  $P$  over Borneo and adjacent waters, a shift southward of the central Pacific ICZ, and less  $P$  over Mexico are linked to higher SLP on the south side of the NP high. A poleward shift of midlatitude storm track and more  $P$  to the south of the high are associated with higher SLP on the north side of the NP high. For higher SLP on the tropical side, the midlatitude storm track is shifted south, suggesting that higher pressures occur on the south side of the NP high owing to movement of the NP high as a whole. The shift of the midlatitude  $P$  is inferred from a dipole pattern because the climatological axis of maximum  $P$  lies between the positive and negative of the dipole in the NP. Generally, these results are consistent with the composite differences. As seen for the SP high, the dominant remote association tends to be that on the corresponding side of the high.

Daily data helped establish the order of events in the associations seen in monthly mean data. To examine associations seen in monthly data, the daily data had to be filtered. To see tropical associations, the filtering had a rather long cutoff period (20 days was used). The filtered daily data seemed to show that 200 hPa VP led the SLP changes more than VP lagged SLP. Decreases in SLP and OLR over the Arabian Sea tend to precede higher SLP over the central portion of the NP high.

Autocorrelation data found some tendency for SLP to be larger first over Central America followed by the southeast side of the high, then followed by the southwest

side of the high into the tropical west Pacific. For a point on the southeast side of the NP high, lowered SLP and OLR over New Guinea as well as higher OLR over Central America preceded higher SLP at the correlation point (by roughly a week). Increased SLP on the southwest side of the NP high was followed by higher OLR in the tropical west Pacific (after roughly a week). Upper level convergence to the north and east of the NP high led higher SLP at the high. The convergence was evident in dipolar patterns of zonal and meridional components of divergent wind at 200 hPa. The meridional wind contribution to the upper level convergence was primarily from enhanced northerly winds northeast of the NP high for points near the climatological high center, even in low-pass filtered data (using a 7-day cutoff).

SLP at various reference points was regressed against a variety of variables (SLP, VP, OLR, skin temperature,  $\theta_{\text{sfc}}$ , 200 hPa meridional divergent wind, etc.). Again, upper level convergence is generally northeast of the reference point and it leads the change at the reference point. (For example, normalized regressed values of 200 hPa meridional divergent wind exceed half a standard deviation in the Gulf of Alaska for a reference point at the NP high center.) Even the filtered data find a prominent middle latitude wave train in SLP, OLR, and other tested fields. Normalized regressed SLP is higher just east of Japan as well as near the reference point. Lower normalized regressed SLP occurs over central Canada and over Indonesia – southeast Asia region. Generally, these lead the SLP at the comparison point. The regressed SLP pattern is consistent with advection of temperature that shows up in normalized regressed values of skin temperature and  $\theta_{\text{sfc}}$ , primarily cooler temperature that develop immediately to the east of the reference point (including western North America) and warmer temperatures that develop over eastern North America; OLR has a similar pattern in those regions. In the tropics, OLR and  $\theta_{\text{sfc}}$  show some evidence for a northward migration of cloudiness from the Indonesian region (4 days lead) to southeast Asia (4 days lag), but the normalized values are only  $\sim 1/4$  of a standard deviation.

The southeast corner has different properties than do other parts of the NP high. SLP southeast of the NP high center is led by higher SLP over a broad region to the east and south of the reference point, encompassing all of Central America. Consistent with that higher pressure, higher OLR ( $>0.4$  standard deviation) over that region leads the SLP change at the comparison point. The higher SLP is associated with higher surface thermal values over Central America (and lower thermal values surrounding the correlation point), though what leads what could not be determined. Higher SLP at the SE reference point appeared to lead both lower OLR across the tropical NP and higher OLR across the tropical SP. The lower OLR near the reference point migrates south and west over time. The SE comparison point was led by reduced OLR in a region surrounding the Bay of Bengal.

An effort was made to test various mechanisms that have been proposed to force or reinforce the NP high. Forcing by warmer than normal continent to the east and colder ocean locally was examined using daily, low-pass filtered surface potential temperature and skin temperature. Colder than average ocean temperatures preceded and remained after stronger SLP, but warmer surface temperatures over the adjacent continent occurred far downstream ( $>60$  degrees longitude) and clearly occurred after the stronger NP high. Indeed, stronger NP high occurred with colder surface temperatures extending inland over much of western North America. Aside from colder surface temperatures locally, the strongest link with SLP variability was forcing by the NP storm track. This forcing was evident as more than simply an extratropical anticyclone merging with or supplanting the subtropical high. The midlatitude forcing was seen in low-pass filtered data and in divergent winds that feed upper level convergence on the east side of the NP high. Forcing by other mechanisms was harder to identify. Forcing by convection over Central America was not observed, indeed the opposite was found: *suppressed* convection (as judged by higher OLR and SLP) was strongly correlated ( $>0.4$  correlation) with subsequent higher SLP in the southeast quadrant of the NP high. (Normalized regression results were similar.) Evidence was mixed for forcing by convection across the western Pacific to Indonesia. Convection in that region, as evident in lowered OLR, preceded higher SLP in the southeast quadrant of the high; evidence being a small though significant correlation ( $>0.2$ ). However, for other points on the tropical side of the NP high the correlations were less strong. For points at the center of the high or higher latitude there was little connection to tropical OLR, except that there was some evidence for lowered OLR over the Arabian Sea roughly a week prior to elevated SLP on the west side of the NP high. Lower values of normalized regressed OLR and SLP over parts of southeast Asia appear to follow higher SLP at the center, west, and northwest parts of the NP high. It is unclear if cloudiness is migrating out of the Indonesian area independent of the NP high or whether intensification of those parts of the NP high drive the convection northward.

The association of NP high SLP with SST was further tested with correlations between climate indices for SOI, Nino 3 + 4, and EOF of the MJO. Contrary to the winter season shown in Grotjahn (2004), ENSO appears little correlated with NP high SLP during summer. SLP on the tropical side of the NP high has some correlation with P and OLR over the western tropical Pacific and Indian Ocean, so one anticipates some influence by the MJO. When the correlations between MJO and SLP show a significant signal, the correlations are notable solely southward of the climatological center of the NP high. Since points at, and to the north of, the NP high center are so strongly influenced by middle latitude systems, the MJO results seem to reinforce a hypothesis that the

NP high is centered between middle latitude and tropical forcing, which are each operating on different timescales.

#### ACKNOWLEDGEMENTS

This work was partially supported by NSF grant 0354545. Mr P. Weir assisted in preparing Figure 1. Dr B. Weare made suggestions regarding the power spectrum calculation. Dr M. Wheeler provided the Wheeler and Hendon MJO EOF coefficients. The NCEP/NCAR Reanalysis 1 data used in this study were provided by the NOAA-CIRES Climate Diagnostics Center, Boulder, Colorado, USA, from their Web site at <http://www.cdc.noaa.gov/>. The authors thank the reviewers for encouraging them to use the regression statistical approach and to consider ENSO forcing. Niño 3 + 4 SST data were obtained from NCEP at the website: <http://www.cpc.ncep.noaa.gov/data/indices/sstoi.indices>. SOI data were obtained from NCEP at the website: <ftp://ftp.ncep.noaa.gov/pub/cpc/wd52dg/data/indices/soi>.

#### REFERENCES

- Chen P, Hoerling M, Dole R. 2001. On the origin of the subtropical anticyclones. *Journal of the Atmospheric Sciences* **58**: 1827–1835.
- Duchon CE. 1979. Lanczos filtering in one and two dimensions. *Journal of Applied Meteorology* **18**: 1016–1022.
- Grotjahn R. 2004. Remote weather associated with south Pacific subtropical sea-level high properties. *International Journal of Climatology* **24**: 823–839.
- Grotjahn R, Immel S. 2001. Observational study of the remote forcing of the Pacific subtropical highs (poster). In *13th Conference on Atmospheric and Oceanic Fluid Dynamics*, Breckenridge, AMS, 16–17.
- Hoskins B. 1996. On the existence and strength of the summer subtropical anticyclones. *Bulletin of the American Meteorological Society* **77**: 1287–1292.
- Kalnay E, Kanamitsu M, Kistler R, Collins W, Deaven D, Gandin L, Iredell M, Saha S, White G, Woollen J, Zhu Y, Leetmaa A, Reynolds R, Chelliah M, Ebisuzaki W, Higgins W, Janowiak J, Mo K, Ropelewski C, Wang J, Jenne R, Joseph D. 1996. The NCEP/NCAR 40-year reanalysis project. *Bulletin of the American Meteorological Society* **77**: 437–471.
- Kiladis GN, Weickmann K. 1992. Circulation anomalies associated with tropical convection during northern winter. *Monthly Weather Review* **120**: 1900–1923.
- Kistler R, Kalnay E, Collins W, Saha S, White G, Woollen J, Chelliah M, Ebisuzaki W, Kanamitsu M, Kousky V, van den Dool H, Jenne R, Fiorino M. 2001. The NCEP/NCAR 50-year reanalysis. *Bulletin of the American Meteorological Society* **82**: 247–267.
- Liu Y, Wu G, Ren R. 2004. Relationship between the subtropical anticyclones and diabatic heating. *Journal of Climate* **17**: 682–698.
- Miyasaka T, Nakamura H. 2005. Structure and formation of the Northern Hemisphere summertime subtropical highs. *Journal of Climate* **18**: 5046–5065.
- Namias J, Clapp P. 1947. Confluence theory of the high tropospheric jet stream. *Journal of Meteorology* **6**: 330–336.
- Press W, Flannery B, Teukolsky S, Vetterling W. 1992. *Numerical Recipes, The Art of Scientific Computing*. Cambridge University Press: New York; 702.
- Rodwell M, Hoskins B. 2001. Subtropical anticyclones and summer monsoons. *Journal of Climate* **14**: 3192–3211.
- Sardeshmukh P, Hoskins B. 1988. The generation of global rotational flow by steady idealized tropical divergence. *Journal of the Atmospheric Sciences* **45**: 1228–1251.
- Seager R, Murtugudde R, Naik N, Clement A, Gordon N, Miller J. 2003. Air-sea interaction and the seasonal cycle of the subtropical anticyclones. *Journal of Climate* **16**: 1948–1966.
- Shaffrey L, Hoskins B, Lu R. 2002. The relationship between the North American summer monsoon, the Rocky Mountains and the North Pacific subtropical anticyclone in HadAM3. *Quarterly Journal of the Royal Meteorological Society* **128**: 2607–2622.
- von Storch H, Zwiers F. 1999. *Statistical Analysis in Climate Research*. Cambridge University Press: Cambridge; 484.
- Wheeler M, Hendon H. 2004. An all-season real-time multivariate MJO index: development of an index for monitoring and prediction. *Monthly Weather Review* **132**: 1917–1932.